Understanding the influence of polymeric ionic liquid sorbent coating substituents on cannabinoid and pesticide affinity in solid-phase microextraction

Victoria R. Zeger, a David S. Bell, and Jared L. Andersona,*

4 5 6

7

10

11

12

13

14

15

16

17

18

19 20

21

22

23

24 25

26

27

28

29

30

31

32

33

1

2

3

^aDepartment of Chemistry, Iowa State University, Ames, Iowa 50011, USA ^bRestek Corporation, 110 Benner Circle, Bellefonte, Pennsylvania 16823, USA

89 Abstract

To understand factors that drive pesticide-cannabinoid selectivity in solid-phase microextraction (SPME), eight new polymeric ionic liquid (PIL) sorbent coatings were designed and compared to four previously reported PIL sorbent coatings for the extraction of pesticides. The four PIL sorbent coatings consisted of either vinylimidazolium or vinylbenzylimidazolium ILs with long alkyl chain substituents (i.e., -C₈H₁₇ or -C₁₂H₂₅) and bis[(trifluoromethyl)sulfonyl]imide ([NTf₂-]) anions, from which the eight new PIL sorbent coatings were adapted. Modifications to the chemical structure of IL monomers and crosslinkers included incorporation of polymerizable p-styrenesulfonate or 3-sulfopropyl acrylate anions, the addition of aromatic moieties, and/or the addition of polar functional groups (i.e., -OH or -O- groups). A total of ten commonly regulated pesticides and six cannabinoids were examined in this study. The effect of salt on the solubility of pesticides and cannabinoids in aqueous solutions was assessed by determining their extraction efficiencies in the presence of varied methanol content. Differences in their solubilities appear to play a dominant role in enhancing pesticide-cannabinoid selectivity. The selectivity, represented as the ratio of pesticide total peak areas to cannabinoid total peak areas, also exhibited a moderate correlation to the affinity of the sorbent coatings towards both the pesticides and the cannabinoids. A positive correlation was observed for the pesticides and a negative correlation was observed for the cannabinoids, suggesting that selectivity was driven by more than the presence of salt in the samples. The sorbent coatings' affinity towards each class of analytes were examined to determine specific interactions that might influence selectivity. The two main structural modifications increasing pesticide-cannabinoid selectivity included the absence of aromatic moieties and the addition of hydrogen bond donor functional groups. Extractions of simple aromatic molecules as probes were performed under similar extraction conditions as the cannabinoids and confirmed the influence of hydrogen bonding interactions on sorbent coating affinity.

Corresponding Author:

- 34 Jared L. Anderson
- 35 Department of Chemistry
- 36 Iowa State University
- 37 Ames, IA 50011
- 38 E-mail address: andersoj@iastate.edu

39 40

41

Keywords: Solid-phase microextraction; Pesticides; Cannabinoids; Polymeric Ionic Liquids; Selectivity

1. Introduction

42

43

44

45

46

47

48

49

50

51

52

53

54

55

56

57

58

59

60

61

62

63

64

65

Ionic liquids (ILs) have become increasingly popular as analyte-selective extraction phases ever since their first use as extraction solvents in 1998 [1]. Their tunable solvation characteristics and designer hydrophobicity has led to their use as solvents and sorbents in microextraction techniques such as single drop microextraction (SDME), dispersive liquid-liquid microextraction (DLLME), and solid-phase microextraction (SPME) [2–4]. SPME is a non-exhaustive extraction technique capable of isolating analytes from sample matrices via an equilibrium process through the distribution of analytes between two phases [5]. Small volume sorbent coatings used in SPME are typically coated or immobilized to a solid support, providing excellent stability during the extraction process allowing the phases to be re-used. Traditional SPME sorbents include (PA), polyethylene glycol (PEG), polydimethylsiloxane polyacrylate (PDMS), PDMS/divinylbenzene (PDMS/DVB), and are capable of extracting a range of polar, mid-polar, and nonpolar analytes [6]. However, novel sorbent coatings and chemistries have been intensely studied in recent years to selectively isolate analytes from complex matrices [7]. Polymeric ionic liquid (PIL) sorbent coatings were first introduced in 2008 to extract esters

Polymeric ionic liquid (PIL) sorbent coatings were first introduced in 2008 to extract esters and fatty acid methyl esters using SPME [8]. These polymers can be designed to be hydrophobic or hydrophilic and consist of IL monomers and/or crosslinkers containing reactive functional groups that can be thermally or photochemically polymerized [8,9]. PIL sorbent coatings can also be immobilized onto a functionalized solid support of silica capillary or metal wire through the use of "on-fiber" polymerization strategies [9,10]. Both linear and crosslinked PIL sorbent coatings have been employed, but crosslinked sorbents have been shown to offer superior thermal and chemical stability, allowing for solvent desorption and use in direct-immersion (DI) SPME [10]. These advancements have led many to investigate the extraction mechanism of PIL sorbent coatings by making structural modifications to the IL monomers and crosslinkers [11,12].

Like ILs, PILs can interact with analytes through multiple interactions, including electrostatic or Coulombic interactions, π - π interactions, hydrophobic or dispersive interactions, dipolar interactions, and hydrogen bonding interactions [13–18]. Meng et al. previously explored the effects of counter anions of cationic PIL networks [13], where poly(1-vinyl-3-hexylimidazolium) PILs paired with either bis[(trifluoromethyl)sulfonyl]imide ([NTf₂-]) or chloride anions were used to extract volatile fatty acids (VFAs) and alcohols using headspace (HS)-SPME. The chloride anion was suspected of interacting with the VFAs and phenols via hydrogen bonding due to its strong hydrogen bond basic behavior. However, analytes with strong intramolecular hydrogen bonding interactions were not thought to interact via hydrogen bonding, but rather only through dispersive interactions [13]. Additionally, the effect of aromatic moieties was studied using the poly(1-4-vinylbenzyl)-3-hexadecylimidazolium [NTf₂-] PIL to extract polyaromatic hydrocarbons (PAHs) [14]. The sorbent coating containing a benzyl moiety provided higher extraction efficiencies and larger partition coefficients for most PAHs, which was believed to be due to π - π interactions. However, these trends were observed in studies where analytes were extracted from the HS of the sample, which may be different from interactions that take place in DI-SPME [19]. In a study by Pacheco-Fernández et al., crosslinked vinylalkyl- and vinylbenzyl- imidazoliumbased PILs were used to extract polar and nonpolar analytes using DI-SPME [15]. Sorbents containing halide anions exhibited higher affinity towards polar analytes, such as bisphenol A, and sorbents consisting of aromatic moieties interacted more strongly towards hydrophobic aromatic molecules, such as naphthalene and carbamazepine. Additionally, a number of crosslinked PIL sorbent coatings have been explored for the extraction of nucleic acids [16]. The cationic polymeric networks were believed to interact with the negatively charged phosphate groups of DNA through electrostatic interactions; the strength of these interactions could be modulated by

66

67

68

69

70

71

72

73

74

75

76

77

78

79

80

81

82

83

84

85

86

87

incorporating different functional groups within the chemical structure of the IL monomer. To explore the possibility of an anion exchange mechanism, a polymerizable anion was incorporated into one of the structures and results indicated that nucleic acids likely undergo exchange with the anions of the sorbent coating [16].

Rather recently, SPME has been employed to develop an analyte-selective extraction method for cannabis matrix components [20–22]. When extracting pesticides using SPME, more polar sorbent coatings such as PA or PDMS/DVB are generally used [6]; meanwhile, more nonpolar sorbent coatings, such as PDMS, are used to extract cannabinoids [21,23]. In a previous study, PIL sorbent coatings were used to develop a method capable of selectively isolating pesticides in the presence of cannabinoids [22]. Previous literature reports suggest that vinylbenzylimidazolium-based PIL sorbent coatings offer high selectivity for low to mid-polarity analytes in the HS [10]; however, high selectivity was observed for mid-polar to nonpolar pesticides when used in the DI-SPME mode. Additionally, the extraction of nonpolar cannabinoids, which co-eluted with some pesticides, was minimized [22]. However, the structural complexity of pesticides and cannabinoids made it challenging to draw strong conclusions about specific interactions taking place between the sorbent coatings and these analytes.

In this work, the structural composition of PIL sorbents was expanded in an effort to identify functional groups that influence PIL extraction behavior. The use of salt in the aqueous sample was shown to play an important role in altering analyte solubilities; however, the affinity of sorbent coatings towards monitored pesticides and cannabinoids was shown to also influence the selectivity of the extraction. It was found that the sorbent coating's affinity towards these pesticides can be increased by using PILs with p-styrenesulfonate ([SS-]) anions, whereas the affinity towards neutral cannabinoids can be increased by using cationic vinylbenzylimidazolium PILs paired with

the [NTf2⁻] anion and functional groups capable of acting as hydrogen bond acceptors (HBAs) into the sorbent's chemical structure. Polymer conformational changes in saturated versus unsaturated salt solutions may also affect the extraction behavior of the sorbent coatings. Additionally, probe molecules consisting of simple aromatic compounds were also analyzed to highlight specific interactions that take place with the sorbent coatings. The hydrogen bonding capabilities of PILs appear to play a role in the sorbent coating's affinity towards certain analytes and can be used to modulate pesticide-cannabinoid selectivity.

2. Experimental

2.1 Reagents and materials

The following reagents were used in the synthesis and purification of IL monomers and crosslinkers: acrylonitrile (≥99%), 1-vinylimidazole (≥99%), imidazole (≥99%), 1-benzylimidazole (99%), triethylene glycol monomethyl ether (m-PEG-3) (≥97.0%), 4-vinylbenzyl chloride (90%), 1-bromooctane (99%), acetonitrile (≥99.9%) and 3-sulfopropyl acrylate potassium salt were obtained from Sigma-Aldrich (St. Louis, MO, USA). Triethanolamine (99%), 1H-benzo[d]imidazole (98%), and sodium 4-vinylbenzenesulfonate (90%) (also known as sodium p-styrenesulfonate ([SS⁻])) were purchased from Oakwood Chemical (Estill, SC, USA). Organic solvents including dichloromethane (DCM) (99.5%), ethyl acetate (99.5%), chloroform (99.8%), dimethyl sulfoxide (≥99.7%), and methanol (99.9%) were obtained from Fisher Scientific (Waltham, MA, USA) as well as sodium hydroxide (95-100.5%) and sodium chloride (≥99%). Additional reagents used in the synthesis of ILs include: 1,12-dibromododecane (98%) from Alfa Aesar (Ward Hill, MA, USA), methane sulfonyl chloride (98%) from ThermoScientific (Waltham, MA, USA), lithium bis[(trifluoromethyl)sulfonyl]imide (LiNTf₂) (>98%) from Tokyo Chemical Industry (TCI) (Tokyo, Japan), 1-octylimidazole (>98%) from Ionic Liquid Technologies

(IoLiTEC) GmbH (Heilbronn, Germany), and 2,6-di-tert-butyl-4-methylphenol (BHT) (99.8%) from Acros Organics (Pittsburgh, PA, USA).

For constructing the SPME fibers, hydrogen peroxide (30% aqueous solution) from Fisher Scientific and vinyltrimethoxysilane (VTMS) (98%) from Acros Organics were used to functionalize the nitinol (NiTi) support wire (127 µm outer diameter) obtained from Nitinol Devices & Components (Fremont, CA, USA). Additional materials included fused silica capillary column (60 m x 0.25 mm) from Sigma-Aldrich and Black and White J-B Weld (Atlanta, GA, USA). The photoinitiator, 2-hydroxyl-2-methylpropiophenone (DAROCUR 1173) (>96%), was obtained from Sigma-Aldrich. The following analytes and reagents were used for extractions: resorcinol (99%) and styrene (99%) were purchased from ThermoScientific; toluene (>99.5%), 4nitroaniline (>99%), 2-chlorophenol (>99%), N,N-dimethylaniline (99%), o-xylene (>99%), mxylene (>99%), p-xylene (>99) were obtained from Sigma-Aldrich; 2-nitrophenol (99%) and 4tert-butyl-phenol (97%) were purchased from Acros Organics and atrazine (98.8%) from Honeywell Fluka (Charlotte, NC, USA). These analytes are referred to as simple probe molecules (SPM). Cannabigerol (CBG), cannabidiol (CBD), cannabinol (CBN), delta-9tetrahydrocannabinol (Δ^9 -THC), delta-8-tetrahydrocannabinol (Δ^8 -THC), cannabichromene (CBC) were obtained from Restek Corporation (Bellefonte, PA, USA) in 1 mL ampules at a concentration of 1000 mg L⁻¹. The Oregon Pesticide Standards (59 pesticides) were also obtained from Restek Corporation. All standards were prepared as a working solution at a concentration of 100 mg L⁻¹. Type I water (18.2 M Ω ·cm) obtained from a MilliQ system from MilliporeSigma was used as the sample matrix for extractions.

2.2 Instrumentation

138

139

140

141

142

143

144

145

146

147

148

149

150

151

152

153

154

155

156

A Varian MR-400 MHz nuclear magnetic resonance (NMR) spectrometer (Palo Alto, CA, USA) or an Avance NEO 400 MHz system with LN2-cooled broadband Prodigy Probe were used to obtain ¹H NMR spectra of purified IL products in deuterated dimethyl sulfoxide from Acros Organics. A Rayonet photochemical reactor (RPR-100) from Southern New England Ultraviolet Company (Brandford, CT, USA) was used for polymerization of the sorbent coating mixtures at 350 nm. An optical microscope was used to ascertain the sorbent coating film thicknesses.

158

159

160

161

162

163

164

165

166

167

168

169

170

171

172

173

174

175

176

177

178

179

180

An Agilent Technologies (Santa Clara, CA, USA) 1260 Infinity HPLC with a variable wavelength detector and 20 µL Rheodyne manual injector was used for successive separation and detection of cannabinoids and simple probe molecules. An identical HPLC system equipped with a diode-array detector was used for the analysis of pesticides. The cannabinoids and SPMs were analyzed on a Restek Raptor ARC-18 column and the pesticides were analyzed on a Restek Raptor biphenyl column. Both analytical columns had dimensions of 150 mm x 4.6 mm I.D. with a 5 μm particle size and were preceded by a guard cartridge (5 mm x 4.6 mm I.D.) with packing identical to the analytical column. Separations were carried out in reverse phase mode using water and acetonitrile (ARC-18) or methanol (Biphenyl) at 1.0 mL/min. The separation methods for the cannabinoids and pesticides were conducted using previously reported methods [22]. The separation of the SPMs increased from 30% acetonitrile to 40% over 3 min and from 40% to 100% organic over 9 min. Solvent composition was held at 100% acetonitrile for 5 min followed by a quick transition back to 30% organic over 3 min. A 5 min hold at 30% acetonitrile was added for column equilibration to yield a total run time of 27 min. Chromatograms are provided in Figures S1 and S2 of the Supplemental Information (SI). Retention times for the SPMs are listed in Table 1.

2.3 Synthesis of ionic liquid monomer and crosslinkers

2.3.1 Synthesis of organic cation component

Synthesis of 1-octyl-3-(4-vinylbenzyl)imidazolium chloride [VBImC₈+][Cl-]. In 5 mL of chloroform, 3 mmol of 1-octylimidazole was reacted with 3.6 mmol of 4-vinylbenzyl chloride in a 100 mL round bottom flask (RBF) at 60 °C for 24 h. The resulting product was dissolved in water and purified with ethyl acetate (10 x 10 mL) using liquid-liquid extraction (LLE). Water was removed under vacuum until dry. The purity of the reaction product was confirmed by ¹H NMR. The synthesis of this IL monomer has been previously reported [14,22].

Synthesis of 1-benzyl-3-(4-vinylbenzyl)imidazolium chloride [VBImBz⁺][Cl⁻] [24]. In 5 mL of acetonitrile, 3.6 mmol of 1-benzylimidazole was reacted with 4.4 mmol of 4-vinylbenzyl chloride in a 100 mL RBF at 80 °C for 36 h. The ionic product was purified and dried as described above.

Synthesis of 1-octyl-3-(4-vinylbenzyl)benzo[d]imidazolium bromide [VBBImCs⁺][CF] [24]. In 15 mL of dimethyl sulfoxide, 8.5 mmol of 1H—benzo[d]imidazole was reacted with 17 mmol of potassium hydroxide for 6 h in a 250 mL RBF at room temperature. Vinylbenzyl chloride (8.5 mmol) was added to the reaction and stirred for 24 h. To purify the reaction, 15 mL of water was added to the solution and was subsequently transferred to a separatory funnel. The product was extracted with chloroform (4 x 10 mL). The combined organic phases were washed with water until a neutral pH was obtained. Chloroform was removed under vacuum and the product was redissolved in 5 mL of acetonitrile. In an additional 2 mL aliquot of acetonitrile, 10.2 mmol of 1-bromooctane was dissolved and allowed to react with 1-(4-vinylbenzyl)benzimidazole at 80 °C for 48 h. Solvent was removed, and the product was washed with diethyl ether (2 x 10 mL) and acetone (4 x 10 mL). The product was then dried under vacuum.

Synthesis of 1-PEG3-3-vinylimidazolium mesylate [VImPEG3⁺][Ms⁻]. The synthetic procedure for vinylimidazolium-based IL monomers containing PEG functionality was previously reported using PEG 4 [25]. In a similar fashion, 6.2 mmol of m-PEG-3 was dissolved in 5 mL of DCM. The 100 mL three-neck flask containing this solution was placed in an ice bath until the solution temperature reached 0 °C. To create the mesylated PEG product, 2.6 mL of triethylamine in 10 mL of DCM was added dropwise via a dropping funnel to facilitate deprotonation followed by a dropwise addition of 6.2 mmol methanesulfonyl chloride dissolved in 10 mL of DCM. The solution was stirred at 0 °C for 45 min and then for 10 h at room temperature. The reaction was transferred to a separatory funnel and quenched by adding 20 mL of 0.1 M HCl. The LLE system was then shaken three times (allowing for phase separation each time) prior to removing the organic layer. The first DCM layer was collected, and the water layer was washed with a second 20 mL of DCM. The combined DCM layer was washed with water (5 x 20 mL) and the solvent was removed under vacuum. In 5 mL of acetonitrile, 1.3 mmol of mesylated PEG was reacted with 1.5 mmol 1-vinylimidazole in a 100 mL RBF at 75 °C for 36 h. The solvent was removed, and the product dissolved in water. Excess 1-vinylimidazole was removed by washing with ethyl acetate $(5 \times 10 \text{ mL}).$ Synthesis of triethanol(4-vinylbenzyl)ammonium chloride [VBTOA+][Cl-] [26]. To obtain [VBTOA⁺][Cl⁻], 3.5 mmol of triethanolamine was reacted with 4.2 mmol of 4-vinylbenzyl chloride in 5 mL of acetonitrile in a 100 mL RBF for 24 h at 80 °C. After removing the solvent, the product was dissolved in water and purified with ethyl acetate (10 x 10 mL).

203

204

205

206

207

208

209

210

211

212

213

214

215

216

217

218

219

220

221

222

Synthesis of 1,12-di(3-(4-vinylbenzyl)imidazolium)dodecane dibromide [VBIm)₂C₁₂+2]2[Br⁻]. The IL crosslinker, [(VBIm)₂C₁₂+2]2[Br⁻], was synthesized following the procedure previously reported [17].

2.3.2 Anion exchange of final IL

Bis[(trifluoromethyl)sulfonyl]imide anion. Certain halide-containing IL monomers and crosslinkers were dissolved in water and reacted with LiNTf₂ in a 1.2 molar excess for monomers or a 2.4 molar excess for crosslinkers to yield products shown in Table 2 [8]. Product 1 was back extracted into ethyl acetate and washed 10 times with water to remove excess salt. Product 2 was extracted back into dichloromethane followed by the same water washing step. The silver nitrate test was conducted on the final washing step to ensure no chloride salts remained.

3-sulfopropyl acrylate anion. The following procedure was used for the preparation of the products based on a previously reported approach [27]. A 1:1 molar equivalent of potassium 3-sulfopropyl acrylate salt was added to the IL monomer in methanol. For IL crosslinkers, a 2:1 molar equivalent was added. The solution was stirred for 24 h at 200 rpm. For products that were soluble in water-immiscible organic solvents, methanol was removed, and the product was redissolved in ethyl acetate or DCM (8 mL) for subsequent washing with water (2 x 8 mL) using LLE. For products that were not soluble in water-immiscible organic solvents, the product was redissolved in acetonitrile and purified by precipitation of the potassium chloride or potassium methanesulfonate by-product. Briefly, the solution was transferred to a 15 mL centrifuge tube, placed in the freezer for 1 h, and then centrifuged for 1 min. The supernatant was collected and evaporated using a stream of air. The resulting product was redissolved in acetonitrile and the freezing and centrifugation steps were repeated until no additional precipitate was observed. Purity was confirmed by NMR, and the spectrum can be found in the SI.

p-styrenesulfonate anion. The anion exchange procedure to incorporate the p-styrenesulfonate anion was obtained from a previously reported method [28]. A 1:1 molar equivalent of sodium p-styrenesulfonate salt was added to the IL monomers (2:1 molar equivalent

for crosslinkers) dissolved in water and was allowed to stir at 200 rpm for 36 hours. The product was back-extracted into ethyl acetate or DCM followed by purification with water. The silver nitrate test was used on the aqueous layer to assess purity followed by NMR. In cases where the product was not soluble in ethyl acetate, the anion exchange procedure was carried out in methanol and was purified by precipitating the inorganic salts, as described for the 3-sulfopropyl acrylate anion. A 1:1 molar equivalent of sodium p-styrenesulfonate salt was added to the IL monomer dissolved in methanol. The solution was allowed to stir for 36 hours before being transferred to a 15 mL centrifuge tube and placed in the freezer for 1 h. The solution was then centrifuged for 1 min and the supernatant was collected. The methanol was removed, and the product was redissolved in acetonitrile. Additional freezing and centrifugation steps were repeated until no precipitate was observed.

2.4 Construction of SPME fibers

SPME fibers were prepared according to a previously reported procedure [10]. The NiTi wire was cut into 2 cm segments, and then placed into a 30% aq. hydrogen peroxide solution which was refluxed at 72 °C for 2 hours. The wires were then removed, rinsed with water, and dried using acetone. The metal was covered with VTMS and heated to 85 °C for 2 h to impart reactive vinyl groups onto the metal surface. The NiTi was removed and cleaned with acetone, followed by drying in a vacuum oven overnight. The subsequent metal supports were kept in a desiccator until needed.

The functionalized NiTi wire was attached to a segment of capillary using J-B Weld epoxy and was cut to a length of 1.2 cm before applying the sorbent coating. The surface of the NiTi wires were cleaned with acetone prior to coating. The specific sorbent coating was weighed out in a 2:1 ratio of monomer to crosslinker by mass. DAROCUR 1173 (photoinitiator) was added as 3% by

total mass of sorbent coating mixture. To homogenize the monomer and crosslinker and photoinitiator, dichloromethane or acetonitrile (depending on their solubilities) was used and then subsequently removed using a stream of air. The sorbent coating mixture was applied to the wire using a glass capillary and polymerized at 350 nm in a photoreactor. All fibers were conditioned in methanol prior to use. Table 3 lists the sorbent coating compositions for all fibers compared in this study as well as their respective film thicknesses. Since PIL sorbent coatings often tend to form droplets, the designated film thickness for a particular sorbent is the average thickness of each droplet. All film thicknesses were determined in the same manner.

2.5 Extraction of simple probe molecules

Extractions of the SPM were conducted to identify interactions that may take place between analytes of interest and the sorbent coatings. These extractions were also used to test the repeatability of the fibers. Conditions were screened to increase the signal response of analytes and obtain complete desorption from the fibers. Prior to each extraction, the fibers were conditioned with methanol for 30 min followed by water for 10 min. The samples for both SPME and TFME methodologies consisted of an aqueous matrix fortified with SPM to a concentration of 400 μ g L⁻¹. The following conditions were used for SPME extractions: extraction time, 60 min; stir rate, 600 rpm; desorption time, 30 min; desorption solvent, 80% MeOH (aq.); desorption volume, 30 μ L. For sorbent coatings capable of anion exchange, 60 mM LiNTf2 was added to the desorption solution. In most cases, two successive desorption steps were required to obtain no detectable carryover from the fibers.

2.6 Extraction of cannabinoids

Extraction conditions from previous studies using PIL sorbent coatings in SPME were used in this work [22,29]. The samples consisted of an analyte concentration of 200 μ g L⁻¹ in pure type I

water. The temperature of the sample was held at room temperature. The fibers were exposed to the sample for 60 min and then desorbed into 30 μ L of methanol using a 15 min desorption step.

2.7 Extraction of pesticides

The optimized conditions from a previous study utilizing PIL sorbent coatings in SPME to selectively extract pesticides from an aqueous matrix were used [22]. The samples consisted of an analyte concentration of 200 μ g L⁻¹ adjusted to pH 2 and contained 30% w/v of sodium chloride. The temperature of the sample was held at 40 °C with a 10 min equilibration time prior to exposing the fibers. The fibers were exposed to the sample for 5 min and then placed in 30 μ L of water for 1 min to rinse the salt off the fiber. The analytes were desorbed into 30 μ L of methanol using a 30 s desorption step.

3. Results and Discussion

3.1 Modifications to the sorbent coating chemical structure

Previously, four imidazolium-based IL sorbent coatings possessing long alkyl chain substituents and/or aromatic moieties paired with [NTf₂-] anions were used to extract pesticides [22]. These sorbent coatings are listed in Table 3 as Fibers **1-4b**. The sorbents showed excellent selectivity towards mid-polar and nonpolar pesticides but failed to extract more polar pesticides. Additionally, the [NTf₂-] anions likely underwent exchange with chloride anions during extractions performed from concentrated sodium chloride solutions; however, significant differences in extraction efficiencies were not observed when extractions were performed before and after the sorbent was exposed to salt solution. These observations catalyzed the design of new classes of sorbent coatings to include polymerizable anions (i.e., [SS-] and [SPA-]) and more polar functional

group substituents (i.e., hydroxyl and ether functional groups), and are also listed in Table 3 as Fibers **A-H**.

By incorporating polymerizable anions within the chemical structures of IL monomers and crosslinkers, both cations and anions should become part of the polymer backbone upon initiation of radical polymerization, and thus, be unable to exchange with ions in solution. This was demonstrated by Feng *et al.* with SPME coatings containing [SS-] anions and benzenesulfonate anions [28]. By adding polar functional groups and substituents to the chemical structure of IL monomers, the resulting sorbent coatings (i.e., Fibers **D-F**) are also more polar. This was validated in a previous study that compared the solubilities of imidazolium [NTf2-]-based ILs in aqueous solutions containing either ether, and/or ester functional groups to ILs without oxygen-containing functional groups [30]. ILs containing oxygen atoms possessed solubilities in aqueous solutions that were one order of magnitude higher, presumably due to the presence of the heteroatoms [30]. Hence, Fibers **D-F** would be expected to have stronger interactions with the aqueous matrix or other polar analytes.

To confirm the aforementioned assumptions, topological polar surface area (TPSA) calculations were conducted on the IL monomers using Chem3D Pro software, and the data is presented in Table 2. TPSA was first introduced by Ertl *et al.* as a faster way to determine molecular polar surface area (MPSA) of a molecule [31]. The TPSA is calculated as the sum of the atomic contribution of each polar fragment/functional group of a molecule. The atomic contribution of many polar functional groups containing N, O, P, and S atoms were predetermined using surface values from numerous molecules and molecule conformations. However, incorporation of P and S containing fragments did not improve the correlation between TPSA and MPSA [32]. The Chem 3D Pro software only considers functional groups containing N and O atoms. Additionally, the 3D

structure is not required for these calculations; only knowledge of the chemical structure is required. These values can even be determined by hand using the atomic PSA contributions given by ref. 31. Examples of the calculation are provided in Figure S3.

The IL monomers of Fibers **D-F** possessed TPSA values ranging from 117.4-144.2 Å² while IL monomers of Fibers **C**, **G** and **H** had TPSA values of 89.8 Å². Additionally, the TPSA value for the IL monomer in Fiber **B** containing [SS⁻] anion was 63.5 Å², which is lower than that of Fiber **C** containing the same cation but the [SPA⁻] anion. Fiber **D** containing [SS⁻] anion had a TPSA value of 117.9 Å², which was also lower than that of Fiber **E** (144.2 Å²) containing the same cation but the [SPA⁻] anion. TPSA values were shown to reflect the hydrogen bonding capability and molecular polarity of a molecule and was a significant descriptor in modeling aqueous solubilities [32]. Therefore, the [SPA⁻] anion appears to make the sorbent coating more polar by increasing the number of HBA groups. The TPSA values for IL monomers containing [NTf₂⁻] anions could not be calculated as the N atom was not defined by the software.

One of the driving features believed to affect the extraction of pesticides is the presence of aromatic moieties within the chemical structure of the sorbent coatings. To gain a better understanding of factors that drive pesticide-cannabinoid selectivity in SPME, IL monomers containing additional aromatic moieties were incorporated in the sorbent coatings (i.e., Fibers G and H). Aromatic functional groups not only interact with other aromatic molecules via π - π interactions, but they can participate in hydrogen bonding interactions [33]. This may allow for better hydration of the sorbent coatings containing aromatic π -systems via hydrogen bonding with water compared to sorbent coatings with aliphatic moieties (lacking aromatic π -systems) [34].

3.2 Influence of salt on the extraction of pesticides and cannabinoids

To understand the influence of specific functional groups comprising the sorbent coating on the extraction of pesticides and cannabinoids, effects of the sample matrix must also be understood. In a previous study, the presence of sodium chloride in the aqueous sample matrix was found to have the largest effect on the selectivity of pesticides [22] – both by "salting out" the pesticides (increased in peak areas) and "salting in" the cannabinoids (decreased in peak areas). The cannabinoids are known to be largely hydrophobic with Log P values above 6, while pesticides span a polarity range from a Log P of 2-7 for those that were able to be extracted (Table S1). Sodium and chloride anions fall near the middle of the Hofmeister series, which has been used to explain the effect of ions on protein solubilities in aqueous solutions, indicating that it can act as either a kosmotrope (water ordering) or chaotrope (water disordering) depending on the analyte [35]. To this extent, it is possible that the salt ions may compete for water molecules that would otherwise interact with the polar functional groups of the pesticides, making them less soluble in the aqueous solution and seemingly more hydrophobic, leading to analyte aggregation [36]. Since cannabinoids are already very hydrophobic, their solubility may actually be improved by disruption of the hydrogen bonding network in water [37,38]. However, this decrease in cannabinoid extraction efficiency with increasing sodium chloride concentration has been observed previously and was attributed to slowed diffusion due to the increased viscosity of the salt solution [39]. Alternatively, the salt may also drive the cannabinoids to adsorb to the glass vial's surface due to poor solubility, resulting in a lower concentration of cannabinoids within the bulk solution of the sample [40].

362

363

364

365

366

367

368

369

370

371

372

373

374

375

376

377

378

379

380

381

382

383

384

To test the solubility of the analytes in the salt solution, varying percentages (0.2-10.2% v/v) of methanol were incorporated into the sample matrix. The results of these experiments are shown in Figures S4 and S5. The addition of a water-miscible organic modifier to the solution (known to

solubilize the analytes of interest) would be expected to improve the solubility of analytes in the aqueous solution. It should also prevent analytes from sorbing to the surface of the glass vial by keeping the analytes in the bulk solution, and thereby, increasing the extraction of analytes that were not previously soluble [40]. It was observed that a decreased amount of pesticides were extracted as the percentage of methanol was increased, indicating the pesticides were still soluble in the salt solution and were not lost to the glass surface. On the contrary, the extraction efficiencies of all cannabinoids increased with increasing content of organic solvent, even up to 10.2% (v/v) of methanol in a salt free aqueous solution. This suggests that the cannabinoids were initially not soluble in the aqueous solution and underwent adsorption to the surface of the glass vial, which was likely amplified by the addition of sodium chloride to the sample matrix.

It is also important to consider the effects that saturated salt solutions can have on the conformation of the sorbent coating polymer network. Many studies have been conducted that quantify the change in the mass of polyelectrolyte brushes in the presence of salt solutions using ellipsometry and/or quartz crystal microbalance with dissipation [38,41–44]. This change in mass has been linked to the influx and outflux of water resulting in swelling and collapsing of the polymer brush [45]. For zwitterionic polymer brushes, which contain a cationic and anionic component within each monomer, the polymer is collapsed in salt-free solution due to inter/intramolecular ion pairing. These inter/intramolecular interactions are disrupted upon exposure to chloride anions, resulting in the swelling of the polymer brush via hydration, making the phase more hydrophilic [41–43]. For cationic polymer brushes, the polymer is considered swelled in salt-free solutions compared to its thickness when dried, and upon exposure to a high concentration of salt with chloride anions (~1 M), the polymer phase collapses due to a loss of water making the polymer more hydrophobic [38]. One study investigated adsorption of malachite

green onto an adsorbent material consisting in part of a polymer brush and noted that the extraction efficiency of malachite green increased when the polymer brush was in a swollen, hydrophilic state. It was assumed that the swollen state improved mass transfer and binding capacity of the material [46]. Therefore, a swelled state of the cationic PIL sorbents in salt-free solutions may favor cannabinoid sorption [47]. Similarly, the swelled state of the zwitterionic-type PIL sorbents containing polymerizable cations and anions at high salt concentrations may favor pesticide sorption, working synergistically with the "salting out" of pesticides and the reduced solubility of the cannabinoids to maximize pesticide-cannabinoid selectivity.

3.3 Factors influencing selectivity of pesticides

To perform a comparison with previously reported work, pesticides were extracted under the reported optimal conditions for Fibers **A-H** and for Fiber **4b**. Fiber **4b** was designed to have a film thickness closer in magnitude to Fibers **1-3** since Fiber **4** from the prior study had a significantly lower film thickness [22]. None of the new sorbent coatings, even those consisting of the more polar IL monomers, were able to extract polar pesticides that eluted before 10 min in the chromatogram, shown in Figure S1. It should be noted that extreme pH conditions may decrease the lifetime of some sorbent coatings. Although the lifetime of the fibers was not assessed in this study, a previous study used PIL sorbent coatings at pH conditions less than 2 for 60 min extraction times, and one fiber was reported to withstand 155 extractions and chemical desorption steps [29]. To define selectivity in a way that can be compared across all sorbent coatings, the total (summed) peak areas of selected mid-polar and nonpolar pesticides were divided by the total peak areas of 6 neutral cannabinoids (CBG, CBD, CBN, Δ^9 -THC, Δ^8 -THC, and CBC). The selected pesticides were chosen to have similar peak areas, and thus are weighted equally, so that the total peak areas were not heavily biased. Additionally, pesticides that eluted at or near the retention times of

cannabinoids were included (pesticides 5-8); these pesticides are listed in Table S1. The affinity of the sorbent coatings towards monitored pesticides was determined by dividing the total peak areas by the film thickness of the sorbent coatings. Previously, the volume has been used to determine sorbent coating affinity [22,48], which is reasonable for comparing sorbent coatings that exhibit similar swelling behavior in aqueous solutions and similar extraction mechanisms. However, sorbents are compared that are expected to have different behavior in aqueous solutions (i.e., polycationic versus polyzwitterionic) as mentioned above. The swelling and collapse of sorbent coating films scale linearly with the dry film thickness but is expected to scale quadratically with volume due to the nature of the volume calculation (i.e., $V = \pi \cdot (d_f^2 + 2d_f r_{core}) \cdot h$ for cylindrical sorbent coatings).

To determine if the sorbent coating's affinity influences the selectivity of pesticide extractions, a scatterplot was generated featuring the affinity for pesticides on the y-axis and selectivity on the x-axis, as shown in Figure 1a. At first observation, a moderately correlated, linearly increasing trend can be observed indicating that the sorbent coating affinity for pesticides does play a role in selectivity rather than selectivity only being dominated by the influence of salt. Upon closer inspection, other trends can be observed within the plot. For instance, there is a linearly increasing trend between pesticide-cannabinoid selectivity and the pesticides' affinity for sorbent coatings containing [NTf2-] anions that have different relative percentages (0, 55, and 100% by mole of imidazolium groups) of aromatic moieties (Fibers 1, 3 and 4). This suggests that sorbent coatings containing fewer aromatic moieties in either the crosslinker or monomer have a higher affinity for pesticides, which influences their selectivity. A linearly increasing trend can be observed in comparing the selectivity of Fiber 4b, Fiber A, and Fiber B. These fibers contain the same IL monomer and crosslinker cations but possess different percentages of [NTf2-] and [SS-] anions.

This suggests that affinities for pesticides increase with the incorporation of polymerizable anions, which also results in increased selectivity. Since the cationic and anionic component of the polymer are both contained within its backbone, it stands to reason that these sorbents may behave similarly to zwitterionic polymers and participate in inter/intramolecular ion pairing. As mentioned previously, increased hydration of the extraction phase due to an influx of ions from solution into the sorbent disrupts intermolecular ion pairing and may favor pesticide mass transfer. Interestingly, no trends could be correlated to differences in the TPSA values of IL monomers.

454

455

456

457

458

459

460

461

462

463

464

465

466

467

468

469

470

471

472

473

474

475

476

To understand factors that influence the extraction of both pesticides and cannabinoids, the affinity for both classes of compounds should be analyzed separately from selectivity, as these effects may get canceled out to some degree or completely. A ranking of the fibers based on their affinities is shown in Figure 1b. The effect of increasing percentages of aromatic moieties (blue color) on sorbent pesticide affinity can be observed following the trend of Fiber 1 > Fiber 3 > Fiber 4. On a similar vein, the affinity decreases (Fiber $\mathbf{H} < \text{Fiber } \mathbf{G} < \text{Fiber } \mathbf{C}$) as their number of aromatic moieties increases (Fiber H \sim Fiber G > Fiber C). This trend fits with the observation noted above, but also suggests that the presence of the alkyl chain plays a role since it was replaced with a terminal benzyl group in Fiber G (compared to Fiber C) but was not replaced in Fiber H. Incorporation of a longer alkyl chain substituent on the imidazolium group for Fiber 2 (pink color) resulted in a decreased sorbent affinity for the pesticides compared to Fiber 1, but only a slight decrease in selectivity was observed. The effect of anion type on the sorbent's affinity for pesticides can also be observed following the trend of Fiber **B** > Fiber **C** > Fiber **4** (orange underlining, green brackets). By comparing fibers with the same cations but different anions (i.e., Fibers **D** and **E**, and separately comparing, Fibers B and C), both fibers containing [SS-] anions produced higher affinities for pesticides than the fibers containing [SPA-] anions (green brackets). Therefore, the

effect of the anion on sorbent affinity for pesticides exhibits the following trend: $[SS^-] > [SPA^-] > [NTf_2^-]$.

3.4 Factors influencing selectivity of cannabinoids

477

478

479

480

481

482

483

484

485

486

487

488

489

490

491

492

493

494

495

496

497

498

499

A similar analysis was applied to the cannabinoids. A scatterplot relating selectivity to the affinity of the sorbent coatings towards cannabinoids is shown in Figure 2a. A linearly decreasing trend is observed between pesticide-cannabinoid selectivity and sorbent affinity for cannabinoids. A closer look at the sorbent coating affinity towards cannabinoids is represented in Figure 2b. Considering Fibers 1, 3, and 4, affinity becomes stronger as the percentage of aromatic moieties within the sorbent coating composition increases (blue color), suggesting that aromatic moieties play a role in extracting cannabinoids. As mentioned above, the opposite trend was observed for the pesticides, indicating that this structural feature may be important for pesticide-cannabinoid selectivity. Another surprising observation is the high affinity of Fiber F towards cannabinoids, as this sorbent was designed to be more polar (teal color). Fiber F exhibited one of the lowest affinities towards the pesticides in this study despite having no aromatic moieties. The PEG functional group of Fiber F is comprised of a PEG group, which can behave as a HBA and may interact with the phenolic moieties of the cannabinoids via hydrogen bonding. As mentioned previously, aromatic moieties can also interact via hydrogen bonding. Therefore, sorbents with HBA functional groups may negatively influence pesticide-cannabinoid selectivity. Additionally, sorbent coatings made with protic IL monomers (Fiber **D** and **E**) may behave as hydrogen bond donors (HBDs), and thus, exhibit weaker interactions with the cannabinoids. This may explain the lower affinities observed for cannabinoids with Fibers **D** and **E** (teal color).

Interestingly, sorbents that have terminal alkyl chains had higher affinities compared to those that have terminal aromatic moieties (Fiber $\mathbf{H} = \text{Fiber } \mathbf{C} > \text{Fiber } \mathbf{G}$) (black color). This behavior

Indicates that the alkyl chain plays a role in extracting cannabinoids. For pesticides, however, Fiber \mathbf{H} had a more similar affinity to Fiber \mathbf{G} than Fiber \mathbf{C} , suggesting that the presence of the aromatic moiety had a greater influence on the extraction of pesticides than the presence of the alkyl chain. These two observations explain the low pesticide-cannabinoid selectivity observed with Fiber \mathbf{H} , which appears to also be more heavily influences by the presence of aromatic moieties than alkyl groups (Fiber \mathbf{H} < Fiber \mathbf{G} < Fiber \mathbf{C} for selectivity). However, for non-aromatic sorbents, an increase in the alkyl chain length resulted in a decrease in sorbent affinity for both pesticides and cannabinoids (pink color), and thus, may have little influence on selectivity for these types of PIL sorbents.

The influence of sorbent coating anions on cannabinoid affinity was opposite that of the pesticides with [NTf2⁻] > [SPA⁻] > [SS⁻] (orange underlining). As mentioned above, the collapsed state of Fibers 1-4 under high salt conditions may have resulted in poor mass transfer and lower binding capacities, leading to lower selectivity of [NTf2⁻]-based sorbents for pesticides. Additionally, the influence of sorbent coating anions on cannabinoid affinity suggests that the anion plays an important role in pesticide-cannabinoid selectivity. The higher affinity observed for Fiber 4 (compared to Fiber B and C) may be due to either the hydrophobicity of the sorbent anion or the state of the polymer during extraction. Since cannabinoid extractions were conducted from salt-free samples, the conformation of the sorbents is different than those expected for pesticide extractions carried out at high salt content. For Fibers 1-4, the sorbents are thought to be more hydrated in salt-free solutions compared to solutions containing high salt concentrations, and Fibers B-H are thought to be more collapsed. The hydration of Fibers 1-4 may lead to a higher binding capacity for the cannabinoids; however, the hydrophilic state may be unfavorable for the hydrophobic cannabinoids. Conversely, the collapsed state of Fibers B-H, presumably due to ion

pairing, would indicate that these phases are more hydrophobic leading to higher extraction efficiencies and higher affinities for cannabinoids [41], but mass transfer may be limited. This may be the reason that the affinities of both polycationic and polyzwitterionic sorbents are more intertwined for the cannabinoids compared to the pesticides. However, the true swelling behavior of these sorbents should be further explored.

3.5 Extraction of simple probe molecules

523

524

525

526

527

528

529

530

531

532

533

534

535

536

537

538

539

540

541

542

543

544

545

The complexity of pesticide and cannabinoid chemical structures makes it challenging to draw conclusions regarding specific interactions that take place with the sorbent coatings. To better understand these interactions, extractions of simpler probe molecules were conducted using the same extraction conditions as the cannabinoids for Fibers A-H. Aromatic compounds with both nonpolar and polar-substituents were analyzed (see Table 1). Since the peak areas are related to the mass of the analyte on the column, which is affected by the molecular weight of the analyte, comparing peak areas or mass extracted between analytes is not an accurate representation of the sorbent affinity. Thus, the data was compared in terms of nanomoles analyte/film thickness (see Figure S6). The mass extracted was determined from the peak areas via an external calibration curve (see Figure S7) and was converted to nanomoles of analyte extracted, which has a direct relationship to the number of molecules extracted. For the five aromatic hydrocarbons (TOL, STY, o-XY, m-XY, and p-XY), of which m-XY and p-XY are considered together, all five analytes exhibited similar affinity towards the sorbent coatings following the order of Fiber A > Fiber C > Fiber $\mathbf{B} > \text{Fiber } \mathbf{D} > \text{Fiber } \mathbf{E} > \text{Fiber } \mathbf{G} > \text{Fiber } \mathbf{H} > \text{Fiber } \mathbf{F}$, as shown in Figure 3. Firstly, Fiber \mathbf{A} containing both [NTf₂-] anions and [SS-] anions in its chemical structure offered the highest affinity for the aromatic hydrocarbons. This could be due to the hydrophobic nature of the [NTf₂-] anion, which has been observed previously [8,13,49]. Fibers with sorbents featuring the [SS-] anion have relatively higher affinities than those containing [SPA⁻] anions. Since the IL monomer of Fiber **B** has a lower calculated TPSA value than the IL monomer of Fiber **C**, the influence of the anion could be one of sorbent hydrophobicity. Additionally, fibers with IL monomers containing HBDs (Fibers **D-E**) provide higher affinities than those with HBAs (Fibers **F-G**). This could be due to the HBDs having stronger hydrogen bonding interactions with the aromatic benzene ring of the analytes. For this to be reasonable, the polymer-solute hydrogen bonding interactions would also need to be more favorable than the water-solute hydrogen bonding interactions [50].

546

547

548

549

550

551

552

553

554

555

556

557

558

559

560

561

562

563

564

565

566

567

568

To better understand the influence of hydrogen bonding on the sorbent affinity, different analytes containing HBDs and/or HBAs were compared, and these are shown in Figure 4. To determine how polar functional groups interact with sorbent coatings, the peak areas of four polar SPMs (RES, 4-NA, 2-CP, and 2-NP) were normalized by the peak area obtained for TOL. By normalizing to TOL, influence pertaining to the aromatic structure is negated as well as the effect of film thickness to some degree, and so, the normalized data represents the affinity of the sorbents towards polar functional groups. RES contains two hydroxyl groups that are meta to each other and has been used as a HBD in deep eutectic solvents [51]. It should be noted that RES has the lowest retention time owing to its high polarity as indicated by its low Log P value of 0.8. It may be for this reason that Fiber A exhibited such a low affinity for this analyte. Additionally, an interesting trend exists for sorbents that contain HBA groups and sorbents that contain HBD groups. Fibers G and F exhibited higher affinities for RES than Fibers E and D, following this order, suggesting that these interactions can play a role in sorbent affinity. It has been previously reported that ILs with [NTf₂] anions have higher enthalpies of hydrogen bonding with protic analytes compared to ILs with sulfonate anions, suggesting that these interactions are more favorable with sulfonate anions [52]. Consequently, the three HBD groups of Fibers **D** and **E** may participate in inter/intramolecular hydrogen bonding with the sulfonate group of the anions, weakening the interaction between the anions and RES.

569

570

571

572

573

574

575

576

577

578

579

580

581

582

583

584

585

586

587

588

589

590

591

Conversely, the probe 2-NP possesses a nitro group and a hydroxyl group and elutes the latest among the four polar-substituted benzenes being analyzed. Based on a previous study, under neutral pH conditions the hydroxyl group of 2-NP molecules in aqueous solutions are believed to be mostly deprotonated [53]. This was further confirmed by the strong electrostatic interactions observed between 2-NP, and to some degree 2-CP, and Fiber A, which is the only sorbent to have exchangeable anions. After many sequential extractions using Fiber A, it was observed that the sorbent changed appearance going from a clear/white color to a bright yellow color, similar to that of the working solution. After a conditioning step in 30 µL of 1 M LiNTf₂ solution (80% methanol aq.), the separation revealed a large amount of 2-NP present, more than had been seen in previous desorptions using only 80% methanol-water solutions (see chromatogram in Figure S8). A noticeable color change back to a whitish-clear color was also observed. The LiNTf2 in the desorption solution likely disrupted the interaction between deprotonated 2-NP molecules and Fiber A and suggests that an ion-exchange mechanism may take place [16]. The deprotonated state of 2-NP eliminates its ability to behave as a HBD. The trend of increasing sorbent affinity follows the order: Fiber $\mathbf{H} >$ Fiber $\mathbf{E} >$ Fiber $\mathbf{C} >$ Fiber $\mathbf{C} >$ Fiber $\mathbf{C} >$ Fiber $\mathbf{F} >$ Fiber \mathbf{A} . Fibers containing the [SS-] anion (Fibers **B** and **D**) have relatively lower affinities for the 2-NP than fibers containing [SPA⁻] anions (Fibers C and E). This trend is also observed for 2-CP, but is not observed for 4-NA and RES, in which Fiber $\mathbf{B} = \text{Fiber } \mathbf{C}$. This could be due to differences in ion pairing strength since electrostatic interactions are believed to occur with these two analytes. One study noted that aromatic sulfonate polymers generally form stronger polyelectrolyte complexes than aliphatic sulfonate polymers [54]. Stronger ion pairing of the [SS-] anion with the cationic

component of the IL may result in weaker electrostatic interaction of 2-NP with the cations compared to PILs containing [SPA⁻] anions. Additionally, sorbents with IL monomers containing HBD functional groups (Fibers **D** and **E**) offered higher affinities than sorbents with HBA functional groups (Fibers **F**).

592

593

594

595

596

597

598

599

600

601

602

603

604

605

606

607

608

609

610

611

612

613

614

To fully understand the extent of hydrogen bonding with PIL sorbent coatings, an examination of more complex analytes containing both HBD (i.e., -OH and -NH₂) and HBA (i.e., -Cl and -NO₂), such as 4-NA and 2-CP, is needed. The order of increasing sorbent affinities for 4-NA follows the order: Fiber $\mathbf{F} = \text{Fiber } \mathbf{G} > \text{Fiber } \mathbf{C} = \text{Fiber } \mathbf{B} > \text{Fiber } \mathbf{E} > \text{Fiber } \mathbf{D} > \text{Fiber } \mathbf{C} > \text{Fibe$ **A.** The order of increasing sorbent affinities for 2-CP follows: Fiber $\mathbf{G} > \text{Fiber } \mathbf{G} > \text{Fiber } \mathbf{B} > \text{Fiber } \mathbf{G} > \mathbf{G$ $\mathbf{H} > \text{Fiber } \mathbf{F} > \text{Fiber } \mathbf{D} > \text{Fiber } \mathbf{A}$. Interestingly, Fiber \mathbf{H} was more highly ranked in terms of affinity for analytes that contain nitro groups (i.e., 4-NA and 2-NP), while Fiber G was more highly ranked for analytes without nitro groups (i.e., RES and 2-CP). Since nitro groups are strong electron withdrawing groups, their greater electron density imparts a partial negative charge onto the functional group; therefore, the nitro groups may better interact with the positively charged benzimidazolium of Fiber H better than the terminal benzyl group of Fiber G. Whereas, for phenolic 2-CP (having a weak electron withdrawing group) and RES, their hydroxy groups can better interact with the terminal benzyl group via hydrogen bonding. As mentioned previously, 2-CP did show some signs of strong electrostatic interactions with Fiber A similar to 2-NP, but to a lesser extent. This is likely due to the higher pKa value (Table 1) of 2-CP (pKa 8.5 ± 0.1) than 2-NP (pKa 7.1 + 0.1), which indicates that less 2-CP molecules are deprotonated at neutral pH 7 conditions compared to 2-NP. Additionally, the ranking for Fibers **D-F** follows Fiber **F** > Fiber **E** > Fiber **D** for RES, 4-NA, and 2-CP, but differs for 2-NP (Fiber **E** > Fiber **D** > Fiber **F**). Therefore, the HBD ability of the molecule seems to play a more important role in facilitating its extraction

with PIL-based sorbent coatings. This may explain why a difference is observed between sorbent coatings containing HBD and HBA groups for cannabinoids, but not for pesticides, which have predominately HBA functional groups.

Conclusions

Eight new crosslinked PIL sorbent coatings were designed in an effort to determine structural features influencing the pesticide-cannabinoid selectivity that had been previously observed in SPME. The structural complexity of the pesticides and cannabinoids makes it challenging to pinpoint specific interactions taking place between these analytes and PIL sorbent coatings; however, by analyzing a total of 12 sorbent coatings, interactions were identified that appear to drive pesticide-cannabinoid selectivity. By analyzing the extraction efficiencies of pesticides and cannabinoids in the presence of various percentages of methanol, it was determined that the influence of salt on selectivity occurred, in part, by reducing the solubility of cannabinoids and leading to adsorption onto the surface of the sample vials. This effect was not observed with the pesticides, resulting in a favorable "salting out" of the pesticides into the sorbent coatings. However, it was also shown that the sorbent coating's affinity towards certain pesticides and cannabinoids played a role in pesticide-cannabinoid selectivity.

The linearly increasing trend observed between the sorbent coatings' affinities for pesticides and pesticide-cannabinoid selectivity and the linearly decreasing trend observed between the sorbent coatings' affinities for cannabinoids and pesticide-cannabinoid selectivity suggests that certain functionalities of the sorbent coating favoring pesticides also disfavor cannabinoids, and vise versa. By ranking the sorbent coatings' affinities for each class of analytes, structural features of the sorbent coating that had opposing effects on the affinities were identified. The incorporation of aromatic moieties in the sorbents favored the extraction of cannabinoids and

disfavored the extraction of pesticides. Additionally, HBA functional groups greatly favored the extraction of cannabinoids. Additionally, the extraction of SPMs showed that the extraction of aromatic hydrocarbons is influenced by the anion type, and to some degree, the HBD/HBA properties of the IL monomer. The extraction of SPMs containing HBD and HBA substituents further supported the influence of hydrogen bonding interactions on the sorbent coatings' affinities. The HBD groups of the analyte also appeared to have a stronger influence on their extraction behavior over HBA groups. Therefore, IL monomers and crosslinkers with HBD groups and lacking aromatic moieties whilst paired with [SS-] anions should be used to maximize pesticide-cannabinoid selectivity.

Acknowledgments

The authors acknowledge partial funding of this work through the Chemical Measurement and Imaging Program at the National Science Foundation (Grant No. CHE-2203891). The authors thank Derek Eitzmann and Dr. Bruce Richter for their valuable input and discussions.

Supporting Information.

Tables containing information regarding the IL monomers and crosslinkers and the monitored pesticides, chromatograms of the pesticide separation and separation of SPMs, graphs showing the effect of organic solvent on the extraction efficiency of pesticides and cannabinoids, graph showing affinities of sorbents towards all SPMs, chromatograms depicting desorption of SPM with LiNTf₂, and ¹H NMR spectra for IL monomers and crosslinkers used to compose PIL sorbent coatings.

References

660

693

694 695

- [1] J.G. Huddleston, H.D. Willauer, R.P. Swatloski, A.E. Visser, R.D. Rogers, Room temperature
 ionic liquids as novel media for 'clean' liquid–liquid extraction, Chem Commun. (1998)
 1765–1766. https://doi.org/10.1039/A803999B.
- [2] J. Liu, G. Jiang, Y. Chi, Y. Cai, Q. Zhou, J.-T. Hu, Use of Ionic Liquids for Liquid-Phase
 Microextraction of Polycyclic Aromatic Hydrocarbons, Anal. Chem. 75 (2003) 5870–5876.
 https://doi.org/10.1021/ac034506m.
- [3] M. García-López, I. Rodríguez, R. Cela, Development of a dispersive liquid–liquid microextraction method for organophosphorus flame retardants and plasticizers determination in water samples, J. Chromatogr. A. 1166 (2007) 9–15.
 https://doi.org/10.1016/j.chroma.2007.08.006.
- [4] J. Liu, N. Li, G. Jiang, J. Liu, J.Å. Jönsson, M. Wen, Disposable ionic liquid coating for headspace solid-phase microextraction of benzene, toluene, ethylbenzene, and xylenes in paints followed by gas chromatography–flame ionization detection, J. Chromatogr. A. 1066 (2005) 27–32. https://doi.org/10.1016/j.chroma.2005.01.024.
- [5] C.L. Arthur, D.W. Potter, K.D. Buchholz, S. Motlagh, J. Pawliszyn, Solid-Phase
 Microextraction for the Direct Analysis of Water: Theory and Practice, LC GC The
 Magazine of Separation Sciences. 10 (1992) 656–661.
- [6] I. Valor, M. Pérez, C. Cortada, D. Apraiz, J.C. Moltó, G. Font, SPME of 52 pesticides and polychlorinated biphenyls: Extraction efficiencies of the SPME coatings poly(dimethylsiloxane), polyacrylate, poly(dimethylsiloxane)-divinylbenzene, Carboxen-poly(dimethylsiloxane), and Carbowax-divinylbenzene, J. Sep. Sci. 24 (2001) 39–48. https://doi.org/10.1002/1615-9314(20010101)24:1<39::AID-JSSC39>3.0.CO;2-2.
- [7] K. Delińska, P.W. Rakowska, A. Kloskowski, Porous material-based sorbent coatings in
 solid-phase microextraction technique: Recent trends and future perspectives, TrAC Trends
 Anal. Chem. 143 (2021) 116386. https://doi.org/10.1016/j.trac.2021.116386.
- [8] F. Zhao, Y. Meng, J.L. Anderson, Polymeric ionic liquids as selective coatings for the extraction of esters using solid-phase microextraction, J. Chromatogr. A. 1208 (2008) 1–9. https://doi.org/10.1016/j.chroma.2008.08.071.
- [9] T.D. Ho, H. Yu, W.T.S. Cole, J.L. Anderson, Ultraviolet Photoinitiated On-Fiber
 Copolymerization of Ionic Liquid Sorbent Coatings for Headspace and Direct Immersion
 Solid-Phase Microextraction, Anal. Chem. 84 (2012) 9520–9528.
 https://doi.org/10.1021/ac302316c.
 - [10] T.D. Ho, B.R. Toledo, L.W. Hantao, J.L. Anderson, Chemical immobilization of crosslinked polymeric ionic liquids on nitinol wires produces highly robust sorbent coatings for solid-phase microextraction, Anal. Chim. Acta. 843 (2014) 18–26. https://doi.org/10.1016/j.aca.2014.07.034.
- [11] D.J.S. Patinha, A.J.D. Silvestre, I.M. Marrucho, Poly(ionic liquids) in solid phase
 microextraction: Recent advances and perspectives, Prog. Polym. Sci. 98 (2019) 101148.
 https://doi.org/10.1016/j.progpolymsci.2019.101148.
- [12] C.M. Graham, Y. Meng, T. Ho, J.L. Anderson, Sorbent coatings for solid-phase
 microextraction based on mixtures of polymeric ionic liquids: Sample Preparation, J. Sep.
 Sci. 34 (2011) 340–346. https://doi.org/10.1002/jssc.201000367.
- 703 [13] Y. Meng, V. Pino, J.L. Anderson, Role of counteranions in polymeric ionic liquid-based solid-phase microextraction coatings for the selective extraction of polar compounds, Anal. Chim. Acta. 687 (2011) 141–149. https://doi.org/10.1016/j.aca.2010.11.046.

706 [14] Y. Meng, J.L. Anderson, Tuning the selectivity of polymeric ionic liquid sorbent coatings 707 for the extraction of polycyclic aromatic hydrocarbons using solid-phase microextraction, J. 708 Chromatogr. A. 1217 (2010) 6143–6152. https://doi.org/10.1016/j.chroma.2010.08.007.

- [15] I. Pacheco-Fernández, A. Najafi, V. Pino, J.L. Anderson, J.H. Ayala, A.M. Afonso, Utilization of highly robust and selective crosslinked polymeric ionic liquid-based sorbent coatings in direct-immersion solid-phase microextraction and high-performance liquid chromatography for determining polar organic pollutants in waters, Talanta. 158 (2016) 125–133. https://doi.org/10.1016/j.talanta.2016.05.041.
- [16] O. Nacham, K.D. Clark, J.L. Anderson, Extraction and Purification of DNA from Complex Biological Sample Matrices Using Solid-Phase Microextraction Coupled with Real-Time PCR, Anal. Chem. 88 (2016) 7813–7820. https://doi.org/10.1021/acs.analchem.6b01861.
- [17] M.D. Joshi, T.D. Ho, W.T.S. Cole, J.L. Anderson, Determination of polychlorinated biphenyls in ocean water and bovine milk using crosslinked polymeric ionic liquid sorbent coatings by solid-phase microextraction, Talanta. 118 (2014) 172–179. https://doi.org/10.1016/j.talanta.2013.10.014.
- [18] J. López-Darias, V. Pino, J.L. Anderson, C.M. Graham, A.M. Afonso, Determination of water pollutants by direct-immersion solid-phase microextraction using polymeric ionic liquid coatings, J. Chromatogr. A. 1217 (2010) 1236–1243. https://doi.org/10.1016/j.chroma.2009.12.041.
- [19] E. Gionfriddo, É.A. Souza-Silva, J. Pawliszyn, Headspace versus Direct Immersion Solid Phase Microextraction in Complex Matrixes: Investigation of Analyte Behavior in Multicomponent Mixtures, Anal. Chem. 87 (2015) 8448–8456. https://doi.org/10.1021/acs.analchem.5b01850.
- [20] S. Giovannoni, C. Lancioni, C. Vaccarini, D. Sedan, D. Andrinolo, C. Castells, Determination of variability of terpenes and terpenoids in Cannabis sativa by gas chromatography-flame ionization detection and gas chromatography-mass spectrometry, J. Chromatogr. A. 1687 (2023) 463669. https://doi.org/10.1016/j.chroma.2022.463669.
- [21] L. Anzillotti, F. Marezza, L. Calò, R. Andreoli, S. Agazzi, F. Bianchi, M. Careri, R. Cecchi, Determination of synthetic and natural cannabinoids in oral fluid by solid-phase microextraction coupled to gas chromatography/mass spectrometry: A pilot study, Talanta. 201 (2019) 335–341. https://doi.org/10.1016/j.talanta.2019.04.029.
- V.R. Zeger, D.S. Bell, J.S. Herrington, J.L. Anderson, Selective isolation of pesticides and cannabinoids using polymeric ionic liquid-based sorbent coatings in solid-phase microextraction coupled to high-performance liquid chromatography, J. Chromatogr. A. 1680 (2022) 463416. https://doi.org/10.1016/j.chroma.2022.463416.
 - [23] Y. Ilias, S. Rudaz, P. Mathieu, P. Christen, J.-L. Veuthey, Extraction and analysis of differentCannabis samples by headspace solid-phase microextraction combined with gas chromatography-mass spectrometry, J. Sep. Sci. 28 (2005) 2293–2300. https://doi.org/10.1002/jssc.200500130.
 - [24] Y. Sarı, A. Aktaş, P. Taslimi, Y. Gök, İ. Gulçin, Novel *N*-propylphthalimide- and 4-vinylbenzyl-substituted benzimidazole salts: Synthesis, characterization, and determination of their metal chelating effects and inhibition profiles against acetylcholinesterase and carbonic anhydrase enzymes, J. Biochem. Mol. Toxicol. 32 (2018) e22009. https://doi.org/10.1002/jbt.22009.

- 751 [25] B. Wu, Z.-W. Zhang, M.-H. Huang, Y. Peng, Polymerizable ionic liquids and polymeric ionic liquids: facile synthesis of ionic liquids containing ethylene oxide repeating unit via methanesulfonate and their electrochemical properties, RSC Adv. 7 (2017) 5394–5401. https://doi.org/10.1039/C6RA26459J.
- T. Wang, W. Wang, Y. Lyu, X. Chen, C. Li, Y. Zhang, X. Song, Y. Ding, Highly
 recyclable polymer supported ionic liquids as efficient heterogeneous catalysts for batch and
 flow conversion of CO ₂ to cyclic carbonates, RSC Adv. 7 (2017) 2836–2841.
 https://doi.org/10.1039/C6RA26780G.
- 759 [27] H.J. Kim, B. Chen, Z. Suo, R.C. Hayward, Ionoelastomer junctions between polymer 760 networks of fixed anions and cations, Science. 367 (2020) 773–776. 761 https://doi.org/10.1126/science.aay8467.

763

764

765

766 767

768

769 770

771

772

773

774

775

780

781

782 783

784

785

786

- [28] J. Feng, M. Sun, L. Xu, S. Wang, X. Liu, S. Jiang, Novel double-confined polymeric ionic liquids as sorbents for solid-phase microextraction with enhanced stability and durability in high-ionic-strength solution, J. Chromatogr. A. 1268 (2012) 16–21. https://doi.org/10.1016/j.chroma.2012.10.037.
 - [29] H. Yu, J. Merib, J.L. Anderson, Crosslinked polymeric ionic liquids as solid-phase microextraction sorbent coatings for high performance liquid chromatography, J. Chromatogr. A. 1438 (2016) 10–21. https://doi.org/10.1016/j.chroma.2016.02.027.
- [30] Y. Deng, P. Besse-Hoggan, M. Sancelme, A.-M. Delort, P. Husson, M.F. Costa Gomes, Influence of oxygen functionalities on the environmental impact of imidazolium based ionic liquids, J. Hazard. Mater. 198 (2011) 165–174. https://doi.org/10.1016/j.jhazmat.2011.10.024.
- [31] P. Ertl, B. Rohde, P. Selzer, Fast Calculation of Molecular Polar Surface Area as a Sum of Fragment-Based Contributions and Its Application to the Prediction of Drug Transport Properties, J. Med. Chem. 43 (2000) 3714–3717. https://doi.org/10.1021/jm000942e.
- 776 [32] Peter Ertl, Polar Surface Area, in: Mol. Drug Prop., WILEY-VCH Verlag GmbH & Co. KGaA, Weinheim, 2008: pp. 111–126.
- 778 [33] Michael Levitt, Max F. Perutz, Aromatic Rings Act as Hydrogen Bond Acceptors, J. Mol. Biol. 201 (1988) 751–754. https://doi.org/10.1016/0022-2836(88)90471-8.
 - [34] G. Graziano, B. Lee, Hydration of Aromatic Hydrocarbons, J. Phys. Chem. B. 105 (2001) 10367–10372. https://doi.org/10.1021/jp011382d.
 - [35] B. Kang, H. Tang, Z. Zhao, S. Song, Hofmeister Series: Insights of Ion Specificity from Amphiphilic Assembly and Interface Property, ACS Omega. 5 (2020) 6229–6239. https://doi.org/10.1021/acsomega.0c00237.
 - [36] A.M. Hyde, S.L. Zultanski, J.H. Waldman, Y.-L. Zhong, M. Shevlin, F. Peng, General Principles and Strategies for Salting-Out Informed by the Hofmeister Series, Org. Process Res. Dev. 21 (2017) 1355–1370. https://doi.org/10.1021/acs.oprd.7b00197.
- 788 [37] S. Moelbert, B. Normand, P. De Los Rios, Kosmotropes and chaotropes: modelling 789 preferential exclusion, binding and aggregate stability, Biophys. Chem. 112 (2004) 45–57. 790 https://doi.org/10.1016/j.bpc.2004.06.012.
- 791 [38] R. Kou, J. Zhang, T. Wang, G. Liu, Interactions between Polyelectrolyte Brushes and 792 Hofmeister Ions: Chaotropes versus Kosmotropes, Langmuir. 31 (2015) 10461–10468. 793 https://doi.org/10.1021/acs.langmuir.5b02698.
- 794 [39] E.S. Emídio, V. de Menezes Prata, H.S. Dórea, Validation of an analytical method for analysis of cannabinoids in hair by headspace solid-phase microextraction and gas

chromatography—ion trap tandem mass spectrometry, Anal. Chim. Acta. 670 (2010) 63–71. https://doi.org/10.1016/j.aca.2010.04.023.

- 798 [40] P.P. Vázquez, A.R. Mughari, M.M. Galera, Application of solid-phase microextraction for determination of pyrethroids in groundwater using liquid chromatography with post-column photochemically induced fluorimetry derivatization and fluorescence detection, J. Chromatogr. A. 1188 (2008) 61–68. https://doi.org/10.1016/j.chroma.2008.02.030.
 - [41] T. Wang, X. Wang, Y. Long, G. Liu, G. Zhang, Ion-Specific Conformational Behavior of Polyzwitterionic Brushes: Exploiting It for Protein Adsorption/Desorption Control, Langmuir. 29 (2013) 6588–6596. https://doi.org/10.1021/la401069y.
 - [42] T. Wang, R. Kou, H. Liu, L. Liu, G. Zhang, G. Liu, Anion Specificity of Polyzwitterionic Brushes with Different Carbon Spacer Lengths and Its Application for Controlling Protein Adsorption, Langmuir. 32 (2016) 2698–2707. https://doi.org/10.1021/acs.langmuir.6b00293.
 - [43] F. Hegaard, R. Biro, K. Ehtiati, E. Thormann, Ion-Specific Antipolyelectrolyte Effect on the Swelling Behavior of Polyzwitterionic Layers, Langmuir. 39 (2023) 1456–1464. https://doi.org/10.1021/acs.langmuir.2c02798.
 - [44] K. Ehtiati, S.Z. Moghaddam, H.-A. Klok, A.E. Daugaard, E. Thormann, Specific Counterion Effects on the Swelling Behavior of Strong Polyelectrolyte Brushes, Macromolecules. 55 (2022) 5123–5130. https://doi.org/10.1021/acs.macromol.2c00411.
 - [45] T. Wang, Y. Long, L. Liu, X. Wang, V.S.J. Craig, G. Zhang, G. Liu, Cation-Specific Conformational Behavior of Polyelectrolyte Brushes: From Aqueous to Nonaqueous Solvent, Langmuir. 30 (2014) 12850–12859. https://doi.org/10.1021/la5033493.
 - [46] Y. Li, X. Feng, Y. Ma, T. Chen, W. Ji, X. Ma, Y. Chen, H. Xu, Temperature and magnetic dual responsive restricted access material for the extraction of malachite green from crucian and shrimp samples, New J. Chem. 44 (2020) 10448–10458. https://doi.org/10.1039/D0NJ00230E.
 - [47] S. Nigam, M. Stephens, A. de Juan, S.C. Rutan, Characterization of the Polarity of Reversed-Phase Liquid Chromatographic Stationary Phases in the Presence of 1-Propanol Using Solvatochromism and Multivariate Curve Resolution, Anal. Chem. 73 (2001) 290–297. https://doi.org/10.1021/ac000836k.
 - [48] D. Orazbayeva, J.A. Koziel, M.J. Trujillo-Rodríguez, J.L. Anderson, B. Kenessov, Polymeric ionic liquid sorbent coatings in headspace solid-phase microextraction: A green sample preparation technique for the determination of pesticides in soil, Microchem. J. 157 (2020) 104996. https://doi.org/10.1016/j.microc.2020.104996.
- [49] J. Merib, H. Yu, E. Carasek, J.L. Anderson, Determination of compounds with varied volatilities from aqueous samples using a polymeric ionic liquid sorbent coating by direct immersion-headspace solid-phase microextraction, Anal. Methods. 8 (2016) 4108–4118. https://doi.org/10.1039/C6AY00423G.
- P. Ruelle, U.W. Kesselring, The Hydrophobic Effect. 3. A Key Ingredient in Predicting n-Octanol-Water Partition Coefficients, J. Pharm. Sci. 87 (1998) 1015–1024. https://doi.org/10.1021/js9703030.
- H. Malaeke, M.R. Housaindokht, H. Monhemi, M. Izadyar, Deep eutectic solvent as an efficient molecular liquid for lignin solubilization and wood delignification, J. Mol. Liq. 263 (2018) 193–199. https://doi.org/10.1016/j.molliq.2018.05.001.
- [52] M.A. Varfolomeev, A.A. Khachatrian, B.S. Akhmadeev, B.N. Solomonov,
 Thermodynamics of hydrogen bonding and van der Waals interactions of organic solutes in

solutions of imidazolium based ionic liquids: "Structure-property" relationships,
Thermochim. Acta. 633 (2016) 12–23. https://doi.org/10.1016/j.tca.2016.03.036.

[53] Y. Ku, K. Lee, W. Wang, Removal of Phenols from Aqueous Solutions by Purolite A-510 Resin, Sep. Sci. Technol. 39 (2005) 911–923. https://doi.org/10.1081/SS-120028453.

[54] J. Fu, H.M. Fares, J.B. Schlenoff, Ion-Pairing Strength in Polyelectrolyte Complexes,
Macromolecules. 50 (2017) 1066–1074. https://doi.org/10.1021/acs.macromol.6b02445.

Figure Legends 848 Figure 1. A. Scatterplot showing the relationship between PIL sorbent coating affinity. 849 represented as the total peak area (TPA) of pesticides divided by the film thickness, and 850 selectivity as the ratio of TPA for the pesticides to the TPA of cannabinoids. Green colored data 851 points represent the polar sorbent coatings determined by TPSA calculations. Orange colored 852 data points represent PIL sorbent coatings with only [NTf₂-] anions. **B.** A list of sorbent coatings 853 based on their affinity towards monitored pesticides. Certain effects are emphasized using 854 855 various colors and underlining. Sorbents with the same color/formatting were compared and the associated effect is indicated in the same color and formatting. 856 Figure 2. A. Scatterplot showing the relationship between PIL sorbent coating affinity (TPA 857 Cannabinoids/Film Thickness) and selectivity (Ratio: Pesticides-to-Cannabinoids). Green 858 859 colored data points represent the polar sorbent coatings determined by TPSA calculations, and 860 orange colored data points represent PIL sorbent coatings with only [NTf₂-] anions. **B.** A list of sorbent coatings based on their affinity towards cannabinoids. Certain effects are emphasized 861 using various colors and underlining. Sorbents with the same color/formatting were compared 862 863 and the associated effect is indicated in the same color and formatting. 864 Figure 3. Bar graph showing the affinity of new PIL sorbent coatings towards aromatic hydrocarbons – toluene (TOL), styrene (STY), and xylenes (o-XY, m-XY, and p-XY). Extraction 865 conditions include concentration of analytes, 400 µg L⁻¹; sample volume, 10 mL DI water; 866 extraction time, 60 min; stir rate, 600 rpm; desorption time, 30 min; desorption solvent, 60 mM 867 868 LiNTf₂ in 80% methanol aq.; desorption volume, 30 μL. Figure 4. Bar graphs (a-d) showing the relative affinity of PIL sorbent coatings towards polar 869 870 functional groups by normalizing the peak areas for each analyte by the peak area of toluene (TOL). Each graph ranks the sorbent coating from lowest to highest affinity. Extraction 871 conditions include concentration of analytes, 400 µg L⁻¹; sample volume, 10 mL DI water; 872 873 extraction time, 60 min; stir rate, 600 rpm; desorption time, 30 min; desorption solvent, 60 mM 874 LiNTf₂ in 80% methanol aq.; desorption volume, 30 μL. 875 876 877 878 879 880 881 882

Table 1. A list of simple probe molecules, their retention times, and computed properties, including Log P and pKa.

| SPM | Rt | Log Pa | pKa ^a |
|-----------------------------|------|------------------|-------------------|
| Resorcinol (RES) | 2.34 | 0.8 ± 0.2 | 9.5 <u>+</u> 0.1 |
| 4-nitroaniline (4-NA) | 4.73 | 1.2 ± 0.2 | 1.0 ± 0.1 |
| 2-nitrophenol (2-NP) | 6.12 | 1.7 ± 0.2 | 7.1 ± 0.1 |
| 2-chlorophenol (2-CP) | 5.59 | 2.2 ± 0.2 | 8.5 ± 0.1 |
| N,N-dimethylaniline (DMA) | 8.03 | 2.1 <u>+</u> 0.2 | 5.1 ± 0.5 |
| Atrazine (ATZ) | 6.64 | 2.6 ± 0.2 | 2.3 ± 0.1 |
| Toluene (TOL) | 8.35 | 2.7 ± 0.2 | n.a. |
| Styrene (STY) | 8.62 | 2.8 ± 0.2 | n.a. |
| o-xylene (o-XY) | 9.20 | 3.2 ± 0.2 | n.a. |
| p-xylene (p-XY) | 9.40 | 3.3 ± 0.2 | n.a. |
| m-xylene (m-XY) | 9.40 | 3.2 ± 0.2 | n.a. |
| 4-tert-butylphenol (4-t-BP) | 7.80 | 3.4 <u>+</u> 0.2 | 10.1 <u>+</u> 0.1 |

a. Obtained from SciFinder and calculated using Advanced Chemistry Development (ACD/Labs) Software V11.02 n.a. not applicable

Table 2. Chemical structures of all IL monomers and crosslinkers used to construct sorbent coatings are shown along with their calculated topological polar surface area (TPSA) values.

| Polymeric Ionic Liquid | Structure | TPSA (Å ²) |
|---|--|------------------------|
| [VBImC ₈ ⁺][NTf ₂ ⁻] | NTf ₂ + | n.c. |
| $[VImC_{8}^{+}][NTf_{2}^{-}]$ | NTI'2.+ | n.c. |
| $[VImC_{12}^{+}][NTf_{2}^{-}]$ | NTf ₂ + | n.c. |
| [VBImC ₈ ⁺][SS ⁻] | | 63.5 |
| [VBImC ₈ ⁺][SPA ⁻] | | 89.8 |
| [VBBzImC ₈ ⁺][SPA ⁻] | | 89.8 |
| [VBImBz ⁺][SPA ⁻] | ************************************** | 89.8 |
| [VBTOA ⁺][SS ⁻] | OH OF OF O | 117.9 |
| [VBTOA ⁺][SPA ⁻] | OH OH OS OF OF | 144.2 |
| [VImPEG3 ⁺][SPA ⁻] | | 117.4 |
| $[(VIm)_2C_{12}^+]2[NTf_2^-]$ | NTf ₂ + C ₁₀ H ₂₀ N + NTf ₂ | n.c. |
| $[(VBIm)_2C_{12}^+]2[NTf_2^-]$ | $\begin{array}{c c} NTf_2 \\ \hline \\ N \end{array} + C_{10}H_{20} \\ \hline \\ N \end{array} $ | n.c. |
| [(VBIm) ₂ C ₁₂ ⁺]2[SS ⁻] | | n.c. |
| [(VBIm) ₂ C ₁₂ ⁺]2[SPA ⁻] | *** C 10H20 N N O O O O | n.c. |

Table 3. Structural composition of sorbent coatings containing IL monomers and IL crosslinkers with their respective labels and film thicknesses obtained using optical microscopy.

| Monomer | Crosslinker | Label | Film Thickness (µm) |
|---|--------------------------------------|----------------|---------------------|
| [VImC ₈ ⁺][NTf ₂ ⁻] | $[(VIm)_2C_{12}^{+2}]2[NTf_2^{-1}]$ | Fiber 1 | 100 |
| $[VImC_{12}^+][NTf_2^-]$ | $[(VIm)_2C_{12}^{+2}]2[NTf_2^{-1}]$ | Fiber 2 | 140 |
| $[VBImC_8^+][NTf_2^-]$ | $[(VIm)_2C_{12}^{+2}]2[NTf_2^{-1}]$ | Fiber 3 | 130 |
| $[VBImC_8^+][NTf_2^-]$ | $[(VBIm)_2C_{12}^{+2}]2[NTf_2^{-1}]$ | Fiber 4b | 150 |
| $[VBImC_8^+][SS^-]$ | $[(VBIm)_2C_{12}^{+2}]2[NTf_2^{-1}]$ | Fiber A | 150 |
| $[VBImC_8^+][SS^-]$ | $[(VBIm)_2C_{12}^{+2}]2[SS^-]$ | Fiber B | 100 |
| $[VBImC_{8}^{+}][SPA^{-}]$ | $[(VBIm)_2C_{12}^{+2}]2[SPA^-]$ | Fiber C | 80 |
| [VBTOA ⁺][SS ⁻] | $[(VBIm)_2C_{12}^{+2}]2[SS^-]$ | Fiber D | 100 |
| [VBTOA ⁺][SPA ⁻] | $[(VBIm)_2C_{12}^{+2}]2[SPA^-]$ | Fiber E | 100 |
| [VImPEG3 ⁺][SPA ⁻] | $[(VBIm)_2C_{12}^{+2}]2[SPA^-]$ | Fiber F | 100 |
| [VBImBz ⁺][SPA ⁻] | $[(VBIm)_2C_{12}^{+2}]2[SPA^-]$ | Fiber G | 100 |
| [VBBzImC ₈ ⁺][SPA ⁻] | $[(VBIm)_2C_{12}^{+2}]2[SPA^-]$ | Fiber H | 100 |

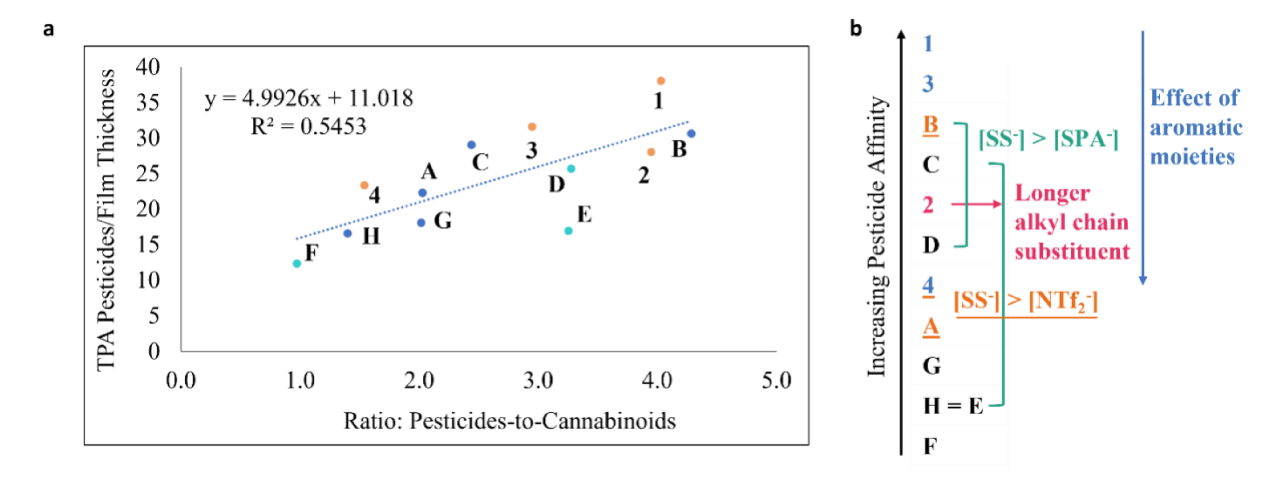


Figure 1. A. Scatterplot showing the relationship between PIL sorbent coating affinity, represented as the total peak area (TPA) of pesticides divided by the film thickness, and selectivity as the ratio of TPA for the pesticides to the TPA of cannabinoids. Green colored data points represent the polar sorbent coatings determined by TPSA calculations. Orange colored data points represent PIL sorbent coatings with only [NTf₂-] anions. **B.** A list of sorbent coatings based on their affinity towards monitored pesticides. Certain effects are emphasized using various colors and underlining. Sorbents with the same color/formatting were compared and the associated effect is indicated in the same color and formatting.

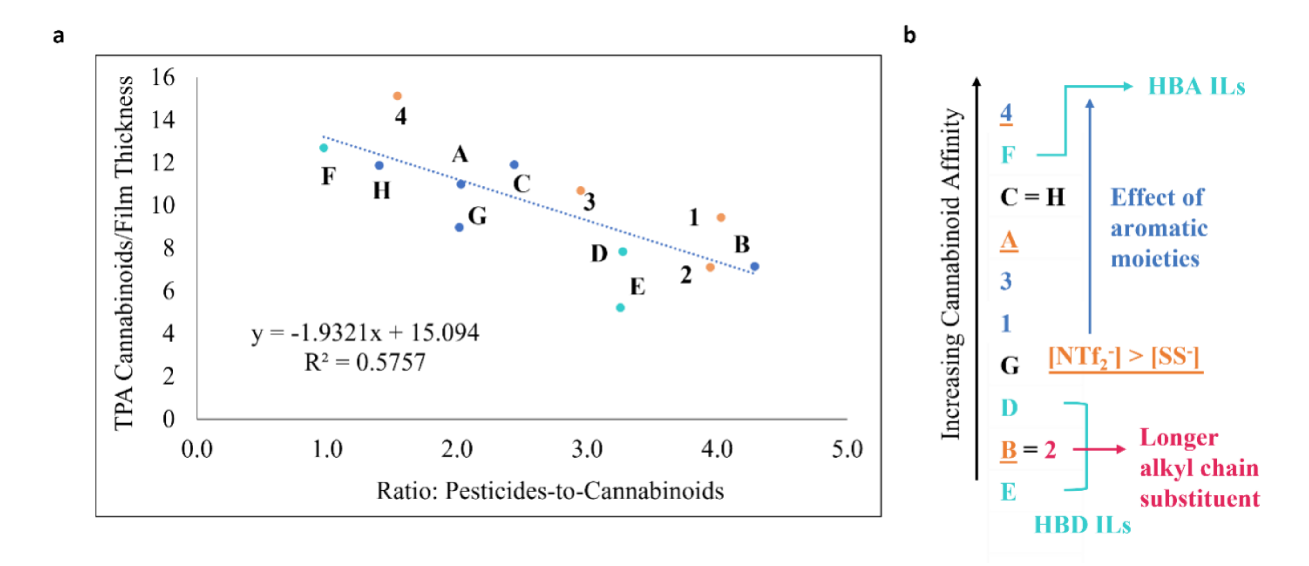


Figure 2. A. Scatterplot showing the relationship between PIL sorbent coating affinity (TPA Cannabinoids/Film Thickness) and selectivity (Ratio: Pesticides-to-Cannabinoids). Green colored data points represent the polar sorbent coatings determined by TPSA calculations, and orange colored data points represent PIL sorbent coatings with only [NTf₂-] anions. **B.** A list of sorbent coatings based on their affinity towards cannabinoids. Certain effects are emphasized using various colors and underlining. Sorbents with the same color/formatting were compared and the associated effect is indicated in the same color and formatting.

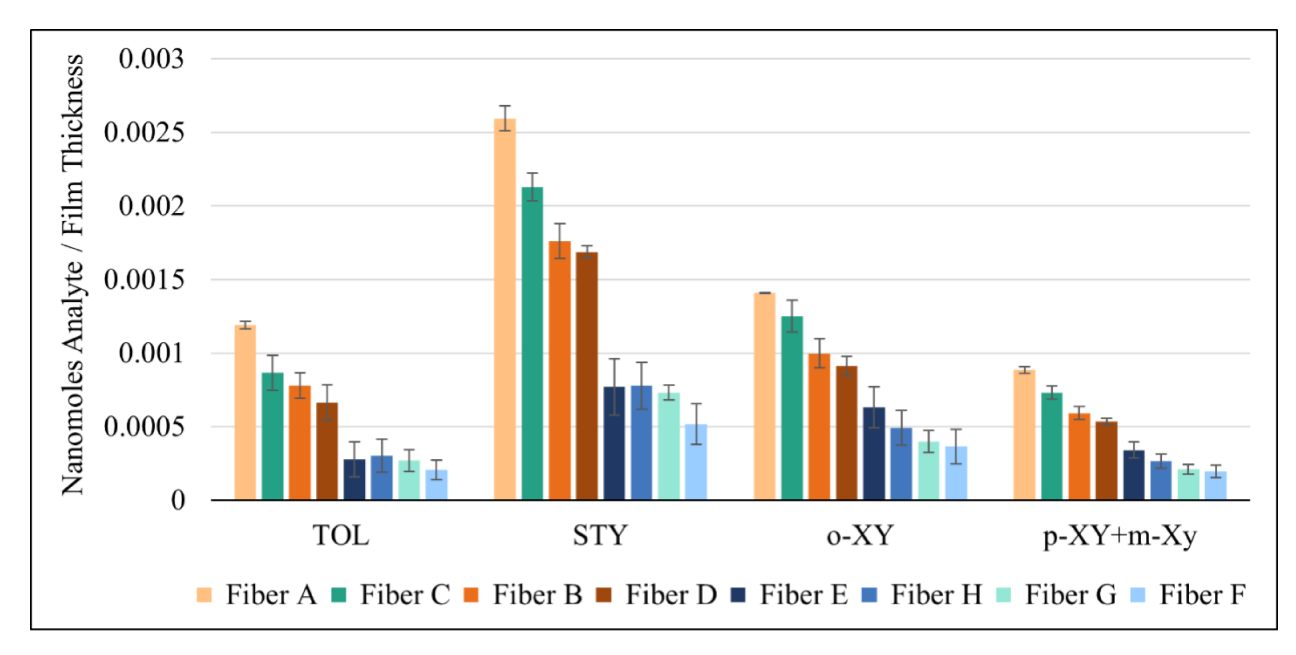


Figure 3. Bar graph showing the affinity of new PIL sorbent coatings towards aromatic hydrocarbons – toluene (TOL), styrene (STY), and xylenes (o-XY, m-XY, and p-XY). Extraction conditions include concentration of analytes, 400 μ g L⁻¹; sample volume, 10 mL DI water; extraction time, 60 min; stir rate, 600 rpm; desorption time, 30 min; desorption solvent, 60 mM LiNTf₂ in 80% methanol aq.; desorption volume, 30 μ L.

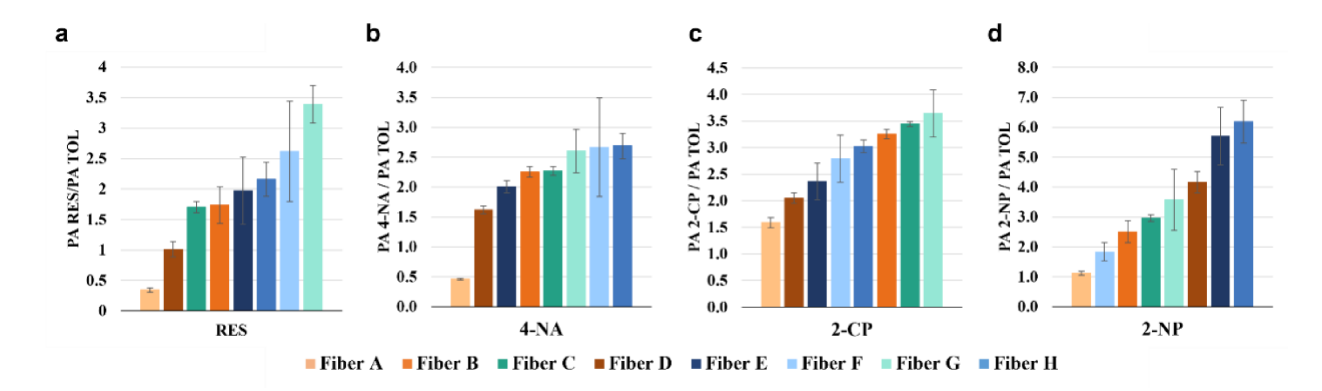


Figure 4. Bar graphs (a-d) showing the relative affinity of PIL sorbent coatings towards polar functional groups by normalizing the peak areas for each analyte by the peak area of toluene (TOL). Each graph ranks the sorbent coating from lowest to highest affinity. Extraction conditions include concentration of analytes, $400~\mu g~L^{-1}$; sample volume, 10~mL DI water; extraction time, 60~min; stir rate, 600~rpm; desorption time, 30~min; desorption solvent, 60~mM LiNTf₂ in 80% methanol aq.; desorption volume, $30~\mu L$.